

## Constraints on deep water age and particle flux in the Equatorial and South Atlantic Ocean based on seawater $^{231}\text{Pa}$ and $^{230}\text{Th}$ data

S. B. Moran<sup>1</sup>, C.-C. Shen<sup>2</sup>, S. E. Weinstein<sup>1</sup>, L. H. Hettlinger<sup>3</sup>, J. H. Hoff<sup>3</sup>, H. N. Edmonds<sup>4</sup> and R. L. Edwards<sup>3</sup>

**Abstract.** High-precision measurements of  $^{231}\text{Pa}$  and  $^{230}\text{Th}$  in filtered seawater and suspended particulate matter samples are reported for the Equatorial and South Atlantic. Distributions of  $^{231}\text{Pa}$  and  $^{230}\text{Th}$  clearly indicate the influence of advection, as evidenced by departures from scavenging models that predict a linear increase with depth for these tracers. Application of a scavenging-mixing model implies a deep water transit time of ~60-100 years from the northern source water regions. The average particulate  $^{231}\text{Pa}/^{230}\text{Th}$  activity ratio is  $0.0498 \pm 0.0160$ , a factor of ~2 lower than the  $^{231}\text{Pa}/^{230}\text{Th}$  production ratio of 0.093 and in agreement with reported excess  $^{231}\text{Pa}/^{230}\text{Th}$  ratios of  $0.06 \pm 0.004$  in Holocene sediments north of  $50^\circ\text{S}$  in the Atlantic. These water column data further suggest that lateral eddy diffusive transport combined with enhanced scavenging in high-particle flux marginal regions (boundary scavenging) is weakly expressed in the Atlantic. Particle fractionation of these tracers is also indicated by the elevated fractionation factors of  $F_{\text{Th/Pa}} = 4.32\text{--}24.04$  (ave. =  $9.97 \pm 4.98$ ) compared to values of ~1-4 in the Southern Ocean.

### Introduction

Sediment studies of the particle-reactive radionuclides  $^{231}\text{Pa}$  (half-life 32 kyr) and  $^{230}\text{Th}$  (half-life 75 kyr), produced by decay of  $^{235}\text{U}$  and  $^{234}\text{U}$ , respectively, have provided new insights into the mode of deep water circulation in the modern and last-glacial Atlantic [Yu et al., 1996]. In contrast to the Pacific [Nozaki and Nakanishi, 1985; Yang et al., 1986], the importance of horizontal advection in redistributing these long-lived tracers in the Atlantic is indicated by low excess sediment  $^{231}\text{Pa}/^{230}\text{Th}$  ratios in both the interior basins and oceans margins north of  $50^\circ\text{S}$  [Yu et al., 1996]. The apparent suppression of boundary scavenging in the Atlantic borne out by the sediment  $^{231}\text{Pa}/^{230}\text{Th}$  ratios has been interpreted as reflecting a similar rate of North Atlantic Deep Water

production during the last glacial period.

An important gap in our understanding of excess sediment  $^{231}\text{Pa}/^{230}\text{Th}$  as a tracer of the large-scale deep water circulation in the modern and last-glacial Atlantic is the paucity of seawater  $^{230}\text{Th}$  and  $^{231}\text{Pa}$  data [Cochran et al., 1987; Rutgers van der Loeff and Berger, 1993; Moran et al., 1995, 1997; Vogler et al., 1998; Walter et al., 1997]. Water column distributions of dissolved and particulate  $^{231}\text{Pa}$  and  $^{230}\text{Th}$  and particulate  $^{231}\text{Pa}/^{230}\text{Th}$  ratios in the contemporary Atlantic are required to constrain the importance of advection and particle fractionation [Walter et al., 1997] for these tracers and hence their use as a proxy for present and past changes in deep water age. In this study, measurements of  $^{231}\text{Pa}$  and  $^{230}\text{Th}$  in filtered water and suspended particulate matter from the Equatorial and South Atlantic are used to constrain the role of advection and scavenging in controlling the distribution of these tracers as they evolve in recently formed, southward flowing, deep waters.

### Methods

Filtered seawater and suspended particulate matter samples were collected in the Equatorial (St. 6;  $8^\circ\text{N}$ ,  $45^\circ\text{W}$ ) and South Atlantic (St. 10;  $33^\circ\text{S}$ ,  $40^\circ\text{W}$ ) during May-June, 1996. Seawater was collected using Go-Flo bottles modified for trace metal sampling and deployed on a Kevlar hydrowire. Seawater was filtered directly from the Go-flo bottles using  $\text{N}_2$  over-pressure through acid-cleaned  $0.4\text{-}\mu\text{m}$ , 90-mm diameter, Teflon filters held in teflon filter holders. Filtered seawater samples (1-2 liters) were stored acidified. Filters containing particulate matter were rinsed with Milli-Q water and stored frozen.

Chemical purification of Pa and Th was conducted using previously described clean techniques [Chen et al., 1986; Edwards et al., 1987, 1997; Moran et al., 1995, 1997; Shen et al., 2000, 2001].  $^{231}\text{Pa}$  and  $^{230}\text{Th}$  abundances were quantified using a Finnigan MAT 262 RPQ thermal ionization mass spectrometer in pulse counting mode.  $^{230}\text{Th}$  was also quantified for particulate samples using a Finnigan MAT ELEMENT sector-inductively plasma mass spectrometer and a CETAC MCN-6000 desolvation nebulizer. Chemical blanks were  $0.47 \pm 0.1$  fg for  $^{230}\text{Th}$  (2-20% of sample) and  $0.016 \pm 0.016$  fg for  $^{231}\text{Pa}$  (1-20% of sample) [Shen et al., 2000]. Uncertainties in the  $^{231}\text{Pa}$  and  $^{230}\text{Th}$  data were calculated at the  $2\sigma$  level and include corrections for blanks, multiplier dark noise, abundance sensitivity, and  $^{231}\text{Pa}$  and  $^{230}\text{Th}$  in the respective  $^{233}\text{Pa}$  and  $^{229}\text{Th}$  spikes.

<sup>1</sup>Graduate School of Oceanography, University of Rhode Island, Narragansett, RI.

<sup>2</sup>Department of Earth Sciences, National Cheng Kung University, Tainan 701, Taiwan, R.O.C.

<sup>3</sup>Department of Geology and Geophysics, University of Minnesota, Minneapolis, MN.

<sup>4</sup>Marine Science Institute, University of Texas at Austin, Port Aransas, TX.

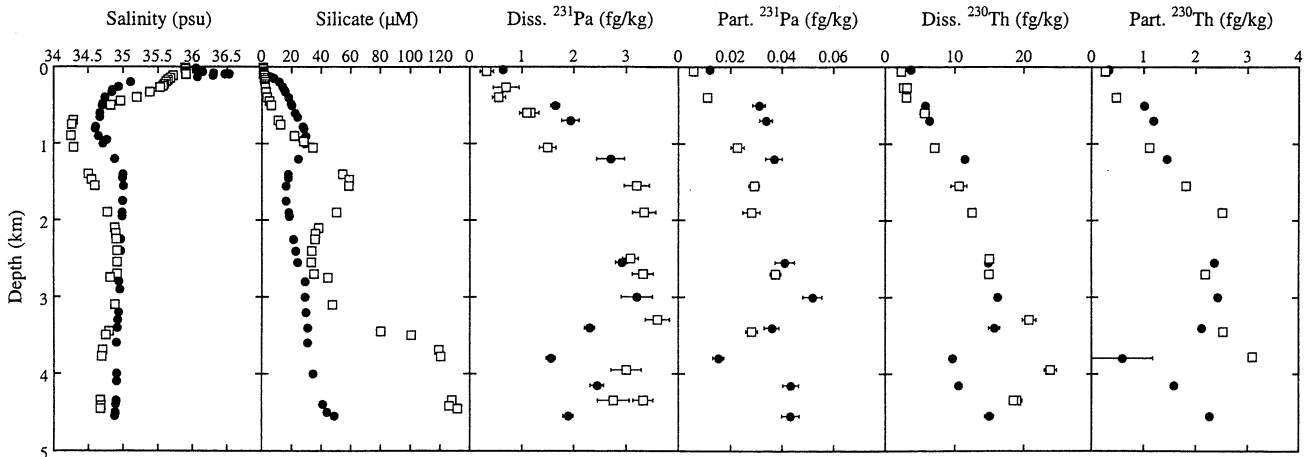


Fig. 1 Depth profiles of salinity, dissolved silicate, and dissolved and particulate  $^{231}\text{Pa}$  and  $^{230}\text{Th}$  concentration in the Equatorial Atlantic ( $\bullet$ , St. 6) and South Atlantic ( $\square$ , St. 10).

## Results

Hydrographic characteristics of St. 6 and St. 10 are illustrated in depth profiles of salinity and dissolved silicate (Fig. 1). As discussed by Cutter and Measures [1999], high-silicate, low-salinity Antarctic Bottom Water (AABW) is evident in the depth range 3950–4460 m at St. 10 and within the bottom 100 m at St. 6. Silicate concentrations are lower above these depths, due to the presence of North Atlantic Deep Water (NADW) between 2200–3200 m at St. 10 and 1600–4200 m at St. 6. Circumpolar Deep Water (CPDW) lies above these depths, as indicated by the elevated silicate concentrations at 1500 m at St. 10 and 1000 m at St. 6. Salinity decreases above this depth into the core of the Antarctic Intermediate Water (AAIW) between  $\sim$ 750–900 m. The upper waters ( $<$ 500 m) at St. 6 and St. 10 are characterized by a salinity maximum and silicate minimum.

Dissolved  $^{231}\text{Pa}$  and  $^{230}\text{Th}$  concentrations (Table 1) range from 0.33–3.61 fg/kg and 2.32–23.88 fg/kg, respectively, and particulate  $^{231}\text{Pa}$  and  $^{230}\text{Th}$  represent approximately 1–2% and 6–20% of the dissolved concentration. The one exception is the sample from the bottom waters at St. 10 (4350 m), where particulate  $^{231}\text{Pa}$  and  $^{230}\text{Th}$  represent, respectively, 9% and 40% of the dissolved fraction, presumably reflecting the importance of resuspended sediment.

Vertical profiles of dissolved  $^{230}\text{Th}$  concentration are characterized by minimum values in the surface waters and a progressive increase with depth to levels of  $\sim$ 15 fg/kg at 2550 m (St. 6) and  $\sim$ 20 fg/kg at 3330 m (St. 10). Below these depths,  $^{230}\text{Th}$  concentrations are increasingly invariant. This is most evident at St. 6, and indeed dissolved  $^{230}\text{Th}$  exhibits a concave distribution within the bottom 1500 m. Dissolved  $^{231}\text{Pa}$  profiles exhibit increasing concentrations from the surface waters down to  $\sim$ 1000–1500 m. Below this depth, dissolved  $^{231}\text{Pa}$  levels are nearly constant and then decrease slightly toward the ocean bottom. As with the distribution of dissolved  $^{230}\text{Th}$ , dissolved  $^{231}\text{Pa}$  concentrations are lower within the bottom  $\sim$ 1500 m at St. 6 compared to values downstream at St. 10. Distributions of particulate  $^{230}\text{Th}$  and  $^{231}\text{Pa}$  concentration closely follow the distribution of the respective dissolved fractions.

$^{230}\text{Th}$  concentrations are within the range of measurements reported for the Norwegian Sea [Moran et al., 1995], Labrador

Sea [Moran et al., 1997], western North Atlantic [Cochran et al., 1987], and the Southern Ocean [Rutgers van der Loeff and Berger, 1993]. Concentrations of  $^{231}\text{Pa}$  are slightly lower than, or similar to, values reported for the Southern Ocean [Rutgers van der Loeff and Berger, 1993]. There are no published Atlantic  $^{231}\text{Pa}$  data north of the stations occupied in this study to compare with our results.

## Discussion

The distributions of  $^{231}\text{Pa}$  and  $^{230}\text{Th}$  clearly indicate departures from scavenging models that predict a linear increase with depth for these tracers. In the case of  $^{230}\text{Th}$ , the majority of oceanographic profiles show an increase with depth throughout the water column, due to production from  $^{234}\text{U}$  and reversible exchange of  $^{230}\text{Th}$  between solution and sinking particles [Bacon and Anderson, 1982; Nozaki et al., 1987; Cochran et al., 1987; Rutgers van der Loeff and Berger, 1993]. These distributions can be explained using a reversible exchange model of Th scavenging [Bacon and Anderson, 1982; Nozaki et al., 1987]. Neglecting diffusive and advective transport, the concentration of total  $^{230}\text{Th}$  is given by  $C_t = (P_{Th}/SK_{Th})z$ , where  $C_t$  is the total  $^{230}\text{Th}$  concentration,  $P_{Th}$  is the  $^{230}\text{Th}$  production rate ( $P_{Th} = 0.56$  fg/kg/y =  $2.8 \times 10^{-5}$  dpm/kg/y),  $S$  is the particle settling rate (m/y),  $K_{Th}$  is the ratio of particulate to total concentration, and  $z$  is water depth. This model has also been applied to  $^{231}\text{Pa}$  [Nozaki and Nakanishi, 1985], however, distributions of  $^{231}\text{Pa}$  typically exhibit a greater degree of variability, ranging from relatively constant values below 1500–2000 m in the Pacific [Nozaki and Nakanishi, 1985] to profiles that increase throughout the water column in the western Arctic [Edmonds et al., 1998].

Several recent water column studies conducted in the North Atlantic indicate the importance of horizontal advection in controlling the distribution of  $^{230}\text{Th}$  in recently formed deep waters. Moran et al. [1997] applied a scavenging-mixing model originally developed by Rutgers van der Loeff and Berger [1993] to explain the low and invariant  $^{230}\text{Th}$  concentrations in the Labrador Sea and Norwegian Sea [Moran et al., 1995], and Vogler et al. [1998] extended this to include results from the eastern North Atlantic. This model can be used to describe the large-scale deep water distributions of

**Table 1.** Salinity, silicate,  $^{231}\text{Pa}$  and  $^{230}\text{Th}$  concentrations, and  $F_{\text{Pa/Th}}$  factors in the Equatorial and South Atlantic.

Depth (m)	Salinity (psu)	Silicate ( $\mu\text{M}$ )	Diss. $^{231}\text{Pa}$ (fg/kg)	Part. $^{231}\text{Pa}$ (fg/kg)	Diss. $^{230}\text{Th}$ (fg/kg)	Part. $^{230}\text{Th}$ (fg/kg)	$F_{\text{Th/Pa}}$
<i>IOC-6, 8°N, 45°W</i>							
40	36.046	1.20	0.64 ± 0.04	0.0121 ± 0.0014	3.65 ± 0.25	0.323 ± 0.03	4.67 ± 0.56
500	34.701	20.11	1.64 ± 0.09	0.0310 ± 0.0024	5.74 ± 0.23	1.014 ± 0.03	9.39 ± 0.60
700	34.949	25.77	1.94 ± 0.17	0.0338 ± 0.0025	6.32 ± 0.18	1.193 ± 0.04	10.86 ± 0.63
1200	34.876	24.39	2.71 ± 0.27	0.0369 ± 0.0033	11.43 ± 0.40	1.449 ± 0.05	9.31 ± 0.85
2550	34.612	23.85	2.92 ± 0.11	0.0411 ± 0.0038	14.87 ± 0.28	2.362 ± 0.05	11.30 ± 0.67
3000	34.942	28.97	3.21 ± 0.30	0.0519 ± 0.0038	16.18 ± 0.40	2.421 ± 0.06	9.25 ± 0.87
3400	34.913	30.68	2.31 ± 0.10	0.0360 ± 0.0029	15.72 ± 0.80	2.116 ± 0.05	8.64 ± 0.98
3800	35.016	23.67	1.56 ± 0.09	0.0154 ± 0.0021	9.64 ± 0.18	0.595 ± 0.59	6.28 ± 0.93
4150	34.923	19.12	2.45 ± 0.13	0.0434 ± 0.0031	10.51 ± 0.24	1.576 ± 0.05	8.47 ± 0.65
4550	34.869	48.67	1.89 ± 0.10	0.0432 ± 0.0035	14.98 ± 0.66	2.263 ± 0.06	6.62 ± 0.90
<i>IOC-10, 33°S, 40°W</i>							
60	35.907	1.33	0.33 ± 0.13	0.0059 ± 0.0014	2.32 ± 0.41	0.265 ± 0.02	6.41 ± 0.75
270	35.530	2.56			2.63 ± 0.39		
270			0.70 ± 0.25		3.13 ± 0.35		
400	35.200	3.74	0.56 ± 0.13	0.0112 ± 0.0016	3.07 ± 0.57	0.478 ± 0.02	7.82 ± 0.85
600	34.285	11.27	1.17 ± 0.16		5.63 ± 0.67		
600			1.10 ± 0.14		5.69 ± 0.41		
1050	34.288	34.58	1.50 ± 0.16	0.0228 ± 0.0025	7.13 ± 0.38	1.119 ± 0.03	10.28 ± 0.76
1550	34.596	58.71	3.21 ± 0.24	0.0292 ± 0.0021	10.62 ± 1.17	1.823 ± 0.04	18.87 ± 1.20
1900	34.780	50.23	3.35 ± 0.22	0.0282 ± 0.0033	12.49 ± 0.47	2.523 ± 0.05	24.04 ± 0.86
2500	34.918	33.20	3.09 ± 0.15		15.07 ± 0.44		
2700	34.916	35.21	3.33 ± 0.20	0.0375 ± 0.0021	15.01 ± 0.45	2.198 ± 0.04	12.98 ± 0.83
3300	34.882	47.57	3.61 ± 0.23		20.77 0.98		
3450	34.801	80.28		0.0282 ± 0.0023		2.532 ± 0.05	
3780	34.694	120.80				3.104 ± 0.06	
3950			3.01 ± 0.29		23.88 ± 0.90		
4350	34.673	128.09	2.76 ± 0.30	0.2592 ± 0.0126	18.98 ± 0.79	7.683 ± 0.08	4.32 ± 1.09
4350			3.33 ± 0.19		18.50 ± 0.50		
4500	34.697			0.3085 ± 0.0572		9.591 ± 0.18	

$^{230}\text{Th}$  and  $^{231}\text{Pa}$  as they evolve in southward flowing, northern source waters. The material balance for total  $^{230}\text{Th}$  and  $^{231}\text{Pa}$  at steady-state is [Rutgers van der Loeff and Berger, 1993; Moran et al., 1997; Vogler et al., 1998],

$$C_t = (P\tau_w + C_i)(1 - e^{-z/\tau_w SK}) \quad (1)$$

where  $C_i$  is the initial  $^{230}\text{Th}$  or  $^{231}\text{Pa}$  concentration in northern source waters,  $\tau_w$  is the water mass age, and the other variables are as described above. For Pa,  $P_{\text{Pa}} = 0.0217$  fg/kg/y ( $2.33 \times 10^{-6}$  dpm/kg/y). The initial  $^{230}\text{Th}$  concentration was set to 4.5 fg/kg [Moran et al., 1997] and  $C_i^{\text{Pa}}$  set to 1 fg/kg (Moran et al., unpublished data). Profiles of total  $^{231}\text{Pa}$  and  $^{230}\text{Th}$  were calculated using the average measured values  $K_{\text{Pa}} = 0.018$  and  $K_{\text{Th}} = 0.14$ . With an estimated particle settling rate of  $S = 500$  m/y, which is within the range of reported values [Bacon and Anderson, 1982; Nozaki and Nakanishi, 1985; Nozaki et al., 1987; Moran et al., 1995, 1997], the calculated depth profiles reproduce the observed linear increase in  $^{231}\text{Pa}$  and  $^{230}\text{Th}$  concentration down to ~1500-2000 m (Fig. 2).

In the deeper waters, both tracers show reasonable agreement with the calculated profiles and imply deep water

ages of ~60-100 years for this portion of the western Atlantic (Fig. 2). Broecker et al. [1991] presented radiocarbon data from 40°N to 30°S that demonstrated rapid ventilation of the western Atlantic and comparatively slower penetration of the tracer into the interior of the ocean. Their contoured ventilation ages for locations corresponding to our stations 6 and 10 are between 80-160 years, in excellent agreement with our results.

The agreement between the observations and the scavenging-mixing model does not rule out the possible removal of these tracers in the deep waters via boundary scavenging; i.e., lateral eddy diffusive transport combined with enhanced scavenging in high-particle flux marginal regions. This would be expected to result in elevated excess sediment  $^{231}\text{Pa}/^{230}\text{Th}$  ratios along the boundaries, however this is inconsistent with results reported by Yu et al. [1996]. In fact, the average  $^{231}\text{Pa}/^{230}\text{Th}$  activity ratio measured on all particulate samples from St. 6 and 10 is  $0.0498 \pm 0.0160$  (Table 1), a factor of ~2 lower than the  $^{231}\text{Pa}/^{230}\text{Th}$  production ratio of 0.093 and in excellent agreement with excess  $^{231}\text{Pa}/^{230}\text{Th}$  ratios of  $0.06 \pm 0.004$  in Holocene sediments from the Atlantic north of 50°S [Yu et al., 1996]. Taken together,

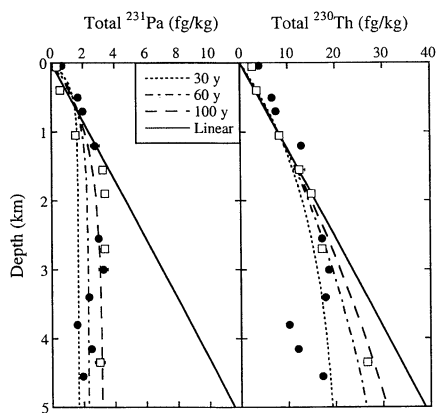


Fig. 2 Depth profiles of total  $^{231}\text{Pa}$  and  $^{230}\text{Th}$  concentration at St. 6 (●) and St. 10 (□) compared with the scavenging-mixing model for  $\tau_w = 30, 60,$  and  $100$  years. Solid line is the linear increase in concentration with depth calculated assuming no advection.

these observations further indicate that boundary scavenging is weakly expressed in the Atlantic as a whole.

Particle composition can also influence particulate  $^{231}\text{Pa}/^{230}\text{Th}$  ratios in the water column and underlying sediments and hence interpretations of boundary scavenging [Anderson et al., 1983; Andersen et al., 1992; Rutgers van der Loeff and Berger, 1993; Walter et al., 1997; Luo and Ku, 1999]. A key question is whether variations in excess sediment  $^{231}\text{Pa}/^{230}\text{Th}$  ratios are caused by boundary scavenging or by preferential removal of  $^{231}\text{Pa}$  or  $^{230}\text{Th}$  by particles with differing particle composition. The degree to which particle composition may affect the fractionation of  $^{231}\text{Pa}$  and  $^{230}\text{Th}$  can be quantified using the fractionation factor

$F_{\text{Th/Pa}}$ ,

$$F_{\text{Th/Pa}} = \frac{\left( \frac{^{230}\text{Th}}{^{231}\text{Pa}} \right)_{\text{part}}}{\left( \frac{^{230}\text{Th}}{^{231}\text{Pa}} \right)_{\text{diss}}} \quad (2)$$

Fractionation factors range from 4.32–24.04 (average =  $9.97 \pm 4.98$ ) (Table 1), clearly indicating particle fractionation of  $^{231}\text{Pa}$  and  $^{230}\text{Th}$  throughout the water column. Also, the measured mean  $F_{\text{Th/Pa}}$  value is coincident with that recently reported by Luo and Ku [1999] for non-biogenic particle phases and greater than  $F_{\text{Th/Pa}} \sim 1$ –4 south of the Antarctic Polar Front [Walter et al., 1997]. The most likely explanation is a greater proportion of silica (opal) in Southern Ocean waters, for which Pa has a higher particle reactivity and hence decreases the fractionation of these tracers [Andersen et al., 1992, Walter et al., 1997].

**Acknowledgments.** We wish to acknowledge the support of the Intergovernmental Oceanographic Commission, the Captain and crew of the R/V *Knorr*, Chief Scientist G. Cutter, and M. Charette and B. Landing for sample collection. This work was funded by the NSF (OCE-9730257 to SBM and HNE; OCE-9731127 and EAR-9712037 to RLE).

## References

- Andersen, H. L., R. Francois, and S. B. Moran, Experimental evidence for differential adsorption of Th and Pa on different particle types in seawater, *Eos, Trans. Amer. Geophys. Union* 73, 270, 1992.
- Anderson, R. F., M. P. Bacon, and P. G. Brewer, Removal of  $^{230}\text{Th}$  and  $^{231}\text{Pa}$  at ocean margins, *Earth Planet. Sci. Lett.*, 66, 73–90, 1983a.

- Bacon, M. P. and R. F. Anderson, Distribution of thorium isotopes between dissolved and particulate forms in the deep sea, *J. Geophys. Res.*, 87, 2045–2056, 1982.
- Broecker, W. S., S. Blanton, W. M. Smethie, Jr., and G. Ostlund, Radiocarbon decay and oxygen utilization in the deep Atlantic Ocean, *Glo. Biogeochem. Cyclic*, 5, 87–117, 1991.
- Chen, J. H., R. L. Edwards, and G. J. Wasserburg,  $^{238}\text{U}$ ,  $^{234}\text{U}$  and  $^{232}\text{Th}$  in seawater, *Earth Planet. Sci. Lett.*, 80, 241–251, 1986.
- Cochran, J. K., H. D. Livingston, D. J. Hirschberg, and L. D. Suprenant, Natural and anthropogenic radionuclide distributions in the northwest Atlantic Ocean, *Earth Planet. Sci. Lett.*, 84, 135–152, 1987.
- Cutter, G. A. and C. I. Measures, The 1996 IOC contaminant baseline survey in the Atlantic Ocean from 33°S to 10°N: introduction, sampling protocols, and hydrographic data, *Deep-Sea Res. II*, 46, 867–884, 1999.
- Edmonds, H. N., S. B. Moran, J. A. Hoff, J. N. Smith and R.L. Edwards, Protactinium-231 and thorium-230 abundances and high scavenging rates in the western Arctic Ocean, *Science* 280, 405–407, 1998.
- Edwards, R. L., H. Cheng, M. T. Murrell and S. J. Goldstein, Protactinium-231 dating of carbonates by thermal ionization mass spectrometry: implications for Quaternary climate change, *Science* 276, 782–786, 1997.
- Edwards, R. L., J. H. Chen, T.-L. Ku and G. J. Wasserburg, Precise timing of the last interglacial period from mass spectrometric determination of Th-230 in corals, *Science*, 236, 1547–1553, 1987.
- Luo, S and T.-L. Ku, Oceanic  $^{231}\text{Pa}/^{230}\text{Th}$  ratio influenced by particle composition and remineralization, *Earth Planet. Sci. Lett.* 167, 183–195, 1999.
- Moran, S. B., J.A. Hoff, K. O. Buesseler and R. L. Edwards, High precision  $^{230}\text{Th}$  and  $^{232}\text{Th}$  in the Norwegian Sea and Denmark Strait by thermal ionization mass spectrometry, *Geophys. Res. Lett.*, 22, 2589–2592, 1995.
- Moran, S. B., M. A. Charette, J. A. Hoff, R. L. Edwards and W. M. Landing, Distribution of  $^{230}\text{Th}$  in the Labrador Sea in relation to ventilation, *Earth Planet. Sci. Lett.* 150 (1/2), 151–160, 1997.
- Nozaki, Y. and T. Nakanishi,  $^{231}\text{Pa}$  and  $^{230}\text{Th}$  in the open ocean water column, *Deep-Sea Res.*, 32(10), 1209–1220, 1985.
- Nozaki, Y., H.-S. Yang, and M. Yamada, Scavenging of thorium in the ocean, *J. Geophys. Res.*, 92 (C1), 772–778, 1987.
- Rutgers van der Loeff, M. M. and G. W. Berger, Scavenging of  $^{230}\text{Th}$  and  $^{231}\text{Pa}$  near the Antarctic Polar Front in the South Atlantic, *Deep-Sea Res.*, 40(2), 339–357, 1993.
- Shen, C.-C., R. L. Edwards, S. B. Moran, S. E. Weinstein, and H. Cheng, Femtogram-sized  $^{230}\text{Th}$  and  $^{231}\text{Pa}$  analyses in seawater by isotope dilution mass spectroscopy, *Eos, Trans. Amer. Geophys. Union*, 81, F620, 2000.
- Shen, C.-C., R. L. Edwards, H. Cheng, J. A. Dorale, R. B. Thomas, S. B. Moran and S. E. Weinstein, Uranium and thorium isotopic concentration measurements by magnetic sector inductively coupled plasma mass spectrometry, *Chem. Geol.* (in review), 2001.
- Vogler, S., J. Scholten, M. M. Rutgers van der Loeff and A. Mangini,  $^{230}\text{Th}$  in the eastern North Atlantic: the importance of water mass ventilation in the balance of  $^{230}\text{Th}$ , *Earth Planet. Sci. Lett.*, 156, 61–74, 1998.
- Walter, H. J., M. M. Rutgers van der Loeff, and H. Hoeltzen, Enhanced scavenging of  $^{231}\text{Pa}$  relative to  $^{230}\text{Th}$  in the South Atlantic south of the Polar Front: Implications for the use of the  $^{231}\text{Pa}/^{230}\text{Th}$  ratio as a paleoproductivity proxy, *Earth Planet. Sci. Lett.*, 149, 85–100, 1997.
- Yang, H. S., Y. Nozaki, H. Sakai and A. Masuda, The distribution of  $^{230}\text{Th}$  and  $^{231}\text{Pa}$  in the deep-sea surface sediments of the Pacific Ocean, *Geochim. Cosmochim. Acta* 50, 81–99, 1986.
- Yu, E.-F., R. Francois and M. P. Bacon, Similar rates of modern and last-glacial ocean thermohaline circulation inferred from radiochemical data, *Nature* 379, 689–694, 1996.

S.B. Moran, S.E. Weinstein, Graduate School of Oceanography, University of Rhode Island, Narragansett, RI 02882-1197.

C.-C. Shen, Department of Earth Sciences, National Cheng Kung University, Tainan 701, Taiwan, R.O.C.

L. H. Hettlinger, J. H. Hoff, R.L. Edwards, Department of Geology and Geophysics, University of Minnesota, Minneapolis, MN 55455.

H.N. Edmonds, Marine Science Institute, University of Texas at Austin, Port Aransas, TX 78373.